Scaffold-Based Three-Dimensional Human Fibroblast Culture Provides a Structural Matrix That Supports Angiogenesis in Infarcted Heart Tissue

Robert S. Kellar, PhD; Lee K. Landeen, MS; Benjamin R. Shepherd, BS; Gail K. Naughton, PhD; Anthony Ratcliffe, PhD; Stuart K. Williams, PhD

Background—We have developed techniques to implant angiogenic patches onto the epicardium over regions of infarcted cardiac tissue to stimulate revascularization of the damaged tissue. These experiments used a scaffold-based 3D human dermal fibroblast culture (3DFC) as an epicardial patch. The 3DFC contains viable cells that secrete angiogenic growth factors and has previously been shown to stimulate angiogenic activity. The hypothesis tested was that a viable 3DFC cardiac patch would stimulate an angiogenic response within an area of infarcted cardiac tissue.

Methods and Results—A coronary occlusion of a branch of the left anterior descending coronary artery was performed by thermal ligation in severe combined immunodeficient mice. 3DFCs with or without viable cells were sized to the damaged area, implanted in replicate mice onto the epicardium at the site of tissue injury, and compared with animals that received infarct surgery but no implant. Fourteen and 30 days after surgery, hearts were exposed and photographed, and tissue samples were prepared for histology and cytochemistry. Fourteen and 30 days after surgery, the damaged myocardium receiving viable 3DFC exhibited a significantly greater angiogenic response (including arterioles, venules, and capillaries) than nonviable and untreated control groups.

Conclusions—In this animal model, viable 3DFC stimulates angiogenesis within a region of cardiac infarction and can augment a repair response in damaged tissue. Therefore, a potential use for 3DFC is the repair of myocardial tissue damaged by infarction. **(*Circulation*. 2001;104:2063-2068.)**

Key Words: angiogenesis ■ ischemia ■ myocardial infarction ■ revascularization

The high incidence and risk of cardiovascular disease have motivated the development of new therapeutic strategies to help treat associated pathologies. Arteriosclerosis is a disease state that affects normal vascular function, and specifically small-caliber arteries such as the coronary arteries. Progression of this disease can result in narrowing or occlusion of the coronary vasculature,[1] ultimately leading to reduced blood flow, induction of areas of cardiac ischemia, and an increased risk of myocardial infarction, in which normal function of the myocardium is compromised.

Surgical interventions include but are not limited to PTCA, CABG, and transmyocardial laser revascularization.[2–5] In addition, angiogenic growth factors (vascular endothelial growth factor [VEGF][6] and basic fibroblast growth factor [bFGF][7]) therapies have been used to stimulate the development of new blood vessels within ischemic cardiac tissues by local or systemic delivery of the protein or gene of interest.[7] A common goal of these interventions is revascularization of damaged or ischemic myocardial tissue with the hope of reducing angina and stimulating recovery of cardiac function. In the study described here, we evaluated a clinically available tissue-engineered device as a cardiac patch to stimulate an angiogenic response within damaged cardiac tissues. The findings suggest that this cardiac patch may be used as a sole therapy or as an adjunct to currently available interventions.

Evaluations of novel angiogenic therapies designed to stimulate revascularization of ischemic or infarcted cardiac tissue have used a variety of animal systems to model the disease state in humans. In the literature, both large-animal (mainly canine and porcine)[8–10] and small-animal (including lupine and rodent)[11–13] models have been used for both acute and chronic models of coronary vessel occlusion. In the acute model, a coronary vessel is occluded by suture ligature, cryoprobe, cautery probe, or microembolization coils,[10,12–14] thereby stimulating an immediate infarction in which intrinsic collateralization of the heart is insufficient to rescue cardiac function and dead cardiomyocytes are replaced by fibrotic scar tissue. Although the infarcted region will grow and the myocardial wall will thin, hibernating cardiomyocytes surrounding the infarcted zone may be temporarily supported nutritionally.

Received May 7, 2001; revision received July 26, 2001; accepted July 31, 2001.

From the Biomedical Engineering Program, University of Arizona, Tucson (R.S.K., B.R.S., S.K.W.), and Advanced Tissue Sciences, Inc, La Jolla, Calif (L.K.L., G.K.N., A.R.).

Correspondence to Dr Stuart K. Williams, Biomedical Engineering Program, University of Arizona, 1501 N Campbell Ave, Tucson, AZ 85724-5084.

Circulation **is available at http://www.circulationaha.org**

The ameroid constrictor represents a widely accepted model of chronic vessel occlusion in large animals,[8,9,15] with more limited use in small animals (rabbits).[16] During this occlusion time (which occurs over weeks rather than years, as in the human condition), cardiomyocytes receive a diminished blood supply and are challenged with an ischemic condition; complete occlusion progresses to an infarct situation. Preinfarction ischemia may allow for intrinsic collateralization of ischemic cardiac tissues even without a treatment modality.

With the acute infarction model used in this study, the contribution of neovascularization from intrinsic collateralization into the infarcted region and the bordering ischemic zone of hibernating myocardium was limited, and the development of new microvessels into the damaged myocardium resulting from the 3D human dermal fibroblast culture (3DFC) implant was augmented. The technique described in this study involves the implantation of a 3DFC cardiac patch over a region of ischemic cardiac tissue to stimulate revascularization of the damaged tissue. 3DFC is a tissue-engineered human dermal fibroblast–derived device that has previously been used for the repair of chronic ulcers.[17] It contains structural extracellular matrix proteins and viable cells that synthesize a number of angiogenic growth factors (including VEGF, bFGF, and hepatocyte growth factor) and has been shown to stimulate angiogenic activity.[18] Although 3DFC has been used in the treatment of chronic leg wounds, this study tested the hypothesis that 3DFC would stimulate an angiogenic response in other wound sites, such as ischemic or infarcted cardiac tissue.

Methods

A matrix-embedded fibroblast culture (Dermagraft) was used throughout the study as the 3DFC. Dermagraft was grown in multicavity bags by seeding human dermal fibroblasts onto 5×7.5-cm pieces of knitted Vicryl mesh (90:10 poly[glycolide:lactide]) and culturing in medium supplemented with serum and ascorbate. At harvest, the medium was replaced with a 10% DMSO-based cryoprotectant, individual bags were separated, and the tissue was frozen and stored at −70°C until required.[17] For the viable 3DFC studies, tissue was rapidly thawed, rinsed, and used immediately. For the nonviable 3DFC implants, tissue was thawed, refrozen for 2 hours without cryoprotectant (lethally damaging existing cells), and rethawed for use in implant studies. Cell viability for both the viable and nonviable 3DFC was confirmed by MTT assay.[18]

Study Design

All animal studies were approved by the University of Arizona animal review committee, and animals were housed in American Association for the Accreditation of Laboratory Animal Care–approved facilities following the procedures of the National Institutes of Health (NIH) *Guidelines for the Care and Use of Laboratory Animals* (NIH publication 85-23, revised 1985). Female, severe combined immunodeficient (SCID) mice weighing 21 to 29 g with induced acute cardiac ischemia received viable 3DFC (n=5) or nonviable 3DFC (n=5) as a single epicardial patch implanted onto the injured site. These treated mice were compared with animals that received coronary occlusion but no implant (n=5). Noninfarcted SCID mice were also used as a control group (n=5). At the time of explantation (14 and 30 days), hearts were injected with an enzymatic marker of nonviable tissue, gross photographs were taken of the injured areas, and samples were processed for general histology and cytochemistry.

Coronary Occlusion and Implant Surgery

General anesthesia was induced and maintained by an intraperitoneal injection of 2.5% Avertin (2.5% 2,2,2-tribromoethanol, 2.5% tert-amyl alcohol in normal saline; Aldrich). Sterility was maintained throughout the procedure. Neck and chest hair was removed with a depilatory agent. A tracheotomy was performed, followed by insertion of a 24-gauge gel catheter to allow for artificial respiration with a ventilator (Harvard Rodent Ventilator model 683) set to deliver 0.9 mL air at 120 breaths/min. Epicardial access was achieved by a left thoracotomy. Occlusion of the first branch of the left anterior descending coronary artery was performed by thermocoagulation,[19] and vessel occlusion was confirmed by a blanching in surface color. Viable 3DFC or nonviable 3DFC patches (4-mm diameter) were sutured (10-0 Prolene suture; Ethicon Corp) onto the epicardial surface over the ischemic region. Mice in the infarct-only treatment group had a coronary occlusion with only the suture implanted. The chest was closed in 3 layers and syringe-evacuated with a 30-gauge needle. Mice were removed from ventilation and recovered under a warming lamp.

Explantation and Evaluation

At the time of explantation (14 or 30 days), general anesthesia was administered with 2.5% Avertin. Hearts were exposed and gross photographs taken after injection of 2% 2,3,5-triphenyltetrazolium chloride (TTC) and incubation at 37°C for 5 minutes. Samples were immediately immersed in Histo-Choice fixative (Ameresco), dehydrated, and embedded in paraffin. Sections (6 μm) were subsequently processed for hematoxylin and eosin (H&E) and cytochemical evaluation.

Sections for cytochemistry were reacted with *Griffonia simplicifolia* lectin (peroxidase-conjugated lectin Gs-1, EY Laboratories; 1:100 final dilution), which binds carbohydrate domains on endothelial cells, and visualized by use of a peroxidase recognition system (Dako, Inc; Universal mouse kit) to identify vascular elements.

Microvessel Density

Gs-1–reacted sections of the damaged epicardium and myocardium affected by the coronary occlusion were observed by light microscopy with a ×40 water-immersion lens. For microvessel density counts, the number of cross-sectional or longitudinal blood-vessel profiles per high-light-magnification area (HLMA, 54×54 μm) were counted and converted to vessels/mm^2.[20] Ten random HLMA counts were taken within the affected tissue. The criteria for positive vessel counts were (1) positive Gs-1 reaction, (2) an identifiable lumen, and (3) within the borders of the designated HLMA. A 1-way ANOVA with Bonferroni post hoc testing was used to determine significance between treatment groups ($P \leq 0.05$).

Microvessel Type Analysis

Sections treated with Gs-1 were analyzed by light microscopy with a ×20 lens. Five random HLMA (200×200 μm) counts were identified within the damaged myocardium (n=5 per group). Microvessels were classified by standard histological features.[21] Capillaries were identified as a single layer of flattened endothelial cells. Arterioles were identified as having an ID ≥10 μm and by the presence of characteristic layers: endothelium, tunica media (consisting of ≥1 smooth muscle layers), and tunica adventitia. Venules were differentiated from arterioles by their large lumen diameter compared with vessel wall thickness, a thinner or absent smooth muscle layer, a less significant tunica adventitia, and an ID >10 μm.

Results

Gross Photography

At explantation, all mouse hearts revealed minimal thoracic adhesions. No recognizable pattern of the adhesive tissue present in infarct-only or 3DFC-treated animals was noted. By gross observation, viable 3DFC-treated mice revealed the highest levels of neovascularization compared with nonviable

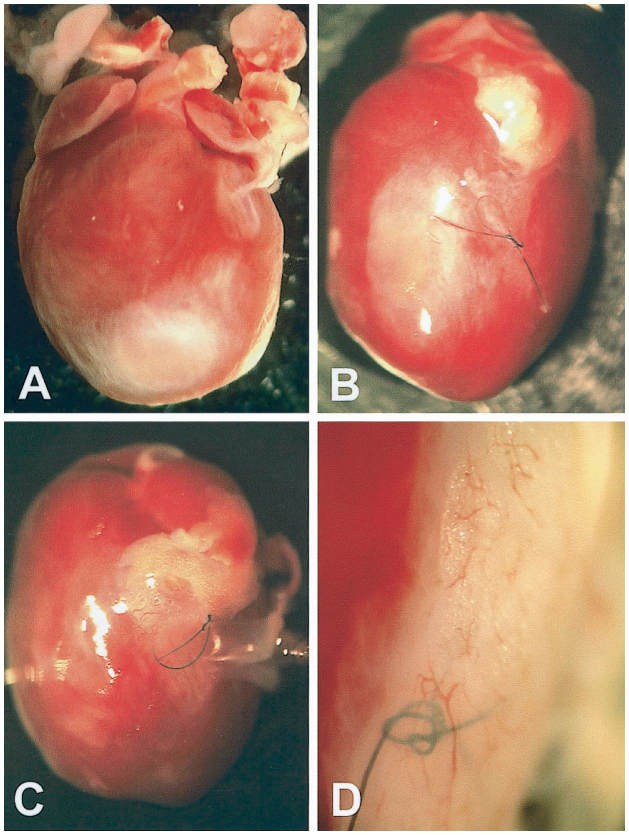

Figure 1. Representative images at time of explantation (14 days) after injection of TTC. A, Infarct-only treatment group. B, Nonviable 3DFC group. C, Viable 3DFC group. D, Higher magnification of viable 3DFC-treated heart (14 days) demonstrating new vasculature.

3DFC and infarct-only mice at the 14- and 30-day time points. Figure 1, a through d, illustrates representative TTC-stained images from 14-day explants in which areas of nonviable tissue are characterized by white (blanched) regions surrounded by dark red, viable cardiac tissue.

Histology and Cytochemistry

At explantation, infarct-only and nonviable 3DFC-treated animals revealed a limited number of new microvessels and the presence of granulation tissue within the damaged myocardium. In contrast, the healing myocardium from viable 3DFC-treated animals demonstrated the presence of new connective tissue and an extensive new microvascular network (Figure 2, a through d). The angiogenic effects of the viable 3DFC material persisted beyond 14 days and was still evident at 30 days.

Vicryl remnants were not observed in all histological samples of 3DFC-treated hearts (viable or nonviable). Inter-animal variability may exist in the degradation rate of the polymer, or histological processing may have facilitated the loss of Vicryl fibers from cross-sectional samples.

Representative images of endothelial stained (Gs-1 lectin) sections and their corresponding serial H&E sections from the 30-day viable 3DFC treatment group (Figure 2, e through h) illustrate the size of the myocardial damage that was observed in serial sections (although not shown in this figure) to extend transmurally.

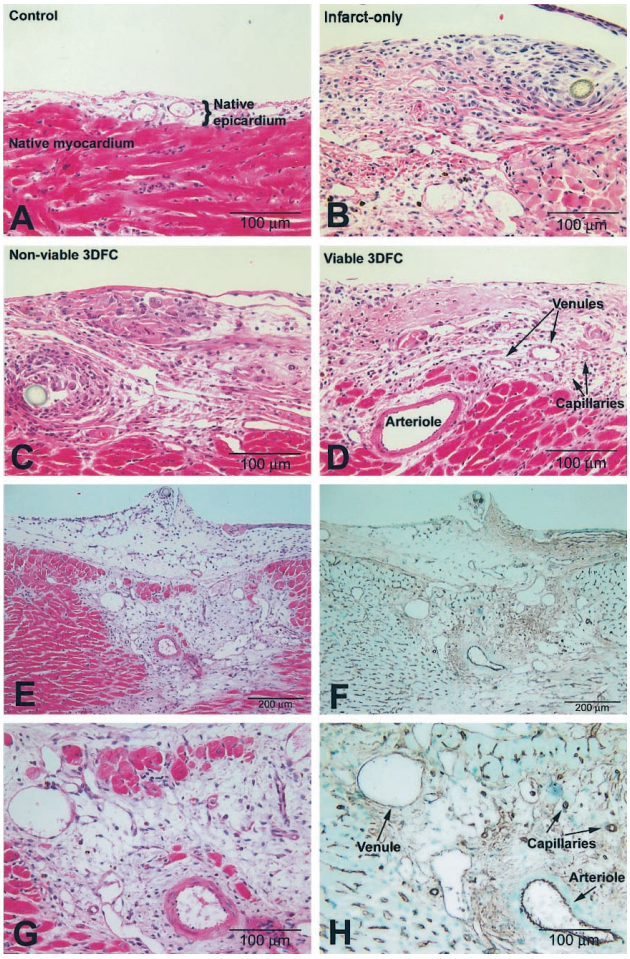

Figure 2. A, H&E histological sections of 14-day heart tissue from control SCID mouse demonstrating normal epicardial and myocardial morphology. B, Infarct-only treatment group. C, Nonviable 3DFC treatment group (suture is visible). D, Viable 3DFC treatment group with new microvessels observed within remodeling cardiac tissue. Microvessels consist of arterioles, capillaries, and venules. E through H, Photographs of H&E sections (E, G) and corresponding serial Gs-1 lectin–reacted sections (F, H) from 30-day viable 3DFC treatment group.

Microvessel Density

Gs-1 lectin–reacted sections were evaluated quantitatively for microvessel densities within the damaged myocardium (Figure 3, a and b). No significant differences were observed between the 2 control treatment groups (infarct-only and nonviable 3DFC) at 14 or 30 days. A significantly greater microvessel density ($P \leq 0.05$) was observed, however, within the damaged area of viable 3DFC-treated mice than in the group treated with nonviable 3DFC or the untreated control group. Microvessel densities of noninfarcted SCID mouse myocardium were calculated (4081 ± 708) for comparison with the 3 treatment groups.

Microvessel Characterization

Further evaluation of Gs-1 lectin–reacted sections provided the relative percentages of arterioles, capillaries, and venules within the damaged myocardium and the average ID of these vessels at both time points (Table). Viable 3DFC treatment resulted in a significantly ($P \leq 0.05$) greater percentage of

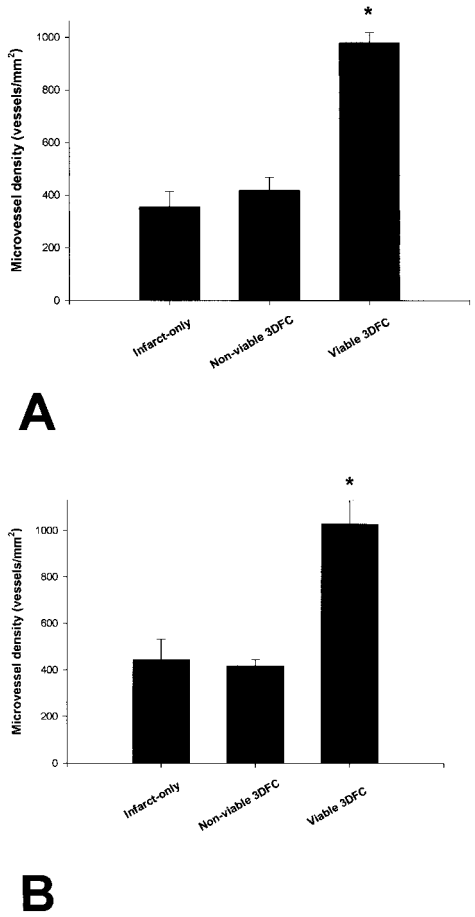

Figure 3. Microvessel densities within damaged myocardium of infarct-only, nonviable 3DFC, and viable 3DFC treatment groups at 14 (A) and 30 (B) days. *$P \leq 0.05$.

arterioles at both 14 and 30 days than in the infarct-only and nonviable 3DFC control groups (Figure 4, a and b).

Depth of Angiogenic Effect of 3DFC

The distance (in micrometers) at which the microvascular effect of the viable 3DFC was attenuated was measured and reported as vessel depth in reference to the ventricular wall thickness at both time points (Figure 5). The border of this effective zone was demarcated by measuring microvessel densities where values became equivalent to the 2 control treatment groups (infarct-only and nonviable 3DFC). In these control groups, there were no identifiable distances from the epicardium at which neovascularization was terminated.

Discussion

These studies demonstrate the ability of a scaffold-based 3DFC to stimulate angiogenesis within an area of cardiac damage. A SCID mouse (lacking functional B and T lymphocytes) model was used for these experiments so as to avoid an immunological tissue-rejection response by the host toward the foreign human fibroblasts. An acute model of myocardial infarction was used in this study to minimize the ability of intrinsic collateralization from ischemic tissues to influence the revascularization of infarcted myocardium. Comparisons of the 3 treatment groups suggest that the angiogenic response was not solely due to a general wound-healing response; the high vascularity within the damaged epicardium and myocardium of the viable 3DFC treatment group was unmatched by the 2 control groups (nonviable 3DFC and infarct-only).

Tissues of the control groups revealed characteristic healing attributes, such as the presence of granulation tissue, fibrous tissue formation, and neovascularization.[22] The local presence of activated macrophages, which have previously been reported to release a variety of angiogenic factors,[23,24] within the granulation tissue or ischemia-induced angiogenesis[25] is a possible explanation for the minimal development of new microvessel sprouts within the myocardium of the control treatment groups. These mechanisms, however, presumably were also present in the damaged hearts of viable 3DFC-treated mice, and the (significant) 2-fold increase in microvessel densities in the 3DFC-treated mice would therefore support a mechanistic response above any commonalities between the treatment groups.

The present data suggest that the angiogenic signals provided by the viable 3DFC material are stimulating the formation of a mature, new vasculature bed with the presence of arterioles, capillaries, and venules. The histological data and subsequent microvessel density measurements demonstrate a greater angiogenic response stimulated by the viable 3DFC than in the control treatment groups. The angiogenic response stimulated by the viable 3DFC was measured to have an effective distance into the damaged myocardium of 310 μm (28.1% across the ventricular wall of 1100 μm) at 14 days and 475 μm (39.6% of 1200 μm) at 30 days. In contrast, the angiogenic sprouts associated with the control treatment groups were primarily capillaries and secondarily venules, and those associated with the nonviable 3DFC group included a minimal percentage of arterioles.

The microvessel density measurements in normal SCID mouse myocardium (4081 ± 708 vessels/mm^2) are consistent with previously reported values for other species (such as rabbit, dog, pig, and human), in which normal microvessel density values range from 3000 to 5000 vessels/mm^2.[15] This finding supports the use of the present methods to determine microvessel density, demonstrates that the values obtained are comparable to those in other species (including humans), and emphasizes that the left anterior descending coronary artery occlusion used in this study dramatically decreased vessel density in the infarcted mice. Previous and current work directed at trying to revascularize damaged myocardium has used various techniques. In the 1930s, the Beck procedure stimulated revascularization of cardiac tissues using an inflammatory/healing response by rubbing the epicardial surface with sandpaper or emery paper.[26] Although an inflammation-mediated response may stimulate angiogenesis, these vessels are supported only as long as the inflammation persists and thus may regress after the resolution of inflammation. More recent studies evaluating new angiogenic therapies in damaged cardiac tissues (including the present study) have accounted for normal granulation tissue vascularity, formed during the inflammatory phase of wound healing, by enrolling control or sham-operated animals.[8,9,12]

Microvessel Characterization, Reported as Percentage of Total, With Average Internal Diameter Measurements (ID. Avg.) at 14 and 30 days

	14 Days			30 Days		
	Arterioles	Capillaries	Venules	Arterioles	Capillaries	Venules
Infarct only						
% of total	0.38%	76.87%	22.75%	0.00%	68.27%	31.73%
SD	0.86%	8.52%	8.12%	0.00%	14.67%	14.67%
ID. Avg., μm	18.00	3.95	18.68	0.00	3.96	21.77
SD	0.00	0.56	3.83	0.00	0.22	3.30
Nonviable 3DFC						
% of total	0.48%	84.33%	11.52%	2.31%	67.35%	30.34%
SD	1.06%	9.06%	3.68%	3.19%	6.46%	9.12%
ID. Avg., μm	10.00	3.58	16.38	19.50	3.92	21.92
SD	0.00	0.27	1.99	8.25	0.38	2.41
Viable 3DFC						
% of total	6.48%	64.84%	28.68%	9.44%	68.11%	22.44%
SD	4.38%	11.20%	13.02%	0.79%	8.33%	9.11%
ID. Avg., μm	11.74	4.26	18.20	10.55	4.11	25.27
SD	6.94	0.83	3.25	0.07	0.65	1.03

Data from the present study suggest that the viable 3DFC material is responsible for the observed and quantified increase in new microvessels within the damaged epicardium and myocardium. This conclusion is supported by previous work in which the angiogenic capacity of 3DFC material has been demonstrated by in vitro tests of endothelial cell proliferation and $\alpha_v\beta_3$ integrin induction,[27] new vessel outgrowth and human vascular endothelial cell motility in rat aortic ring assays,[28] and use of in vivo tests of the chick chorioallantoic membrane.[27] Additional clinical studies to assess the healing of diabetic foot ulcers[29] after treatment with allogeneic, viable 3DFC material have further demonstrated the angiogenic ability of this tissue-engineered material in subjects with functional immune systems and suggest that viable 3DFC maintains its angiogenic effect with a negligible host immune response. Therefore, in light of the previously reported angiogenesis data in both in vitro and in vivo models, we anticipated that an angiogenic effect in an immune-incompetent animal similar to that seen in studies in immune-competent, allogeneic humans would take place and that angiogenic effects of viable 3DFC would be functional in other tissues, including damaged myocardium of the heart.

The mechanism responsible for the neovascularization observed in this study is currently unknown. A possible explanation is the angiogenic milieu that viable 3DFC is known to release. Viable 3DFC material has been characterized to produce a heterogeneous population of cytokines,

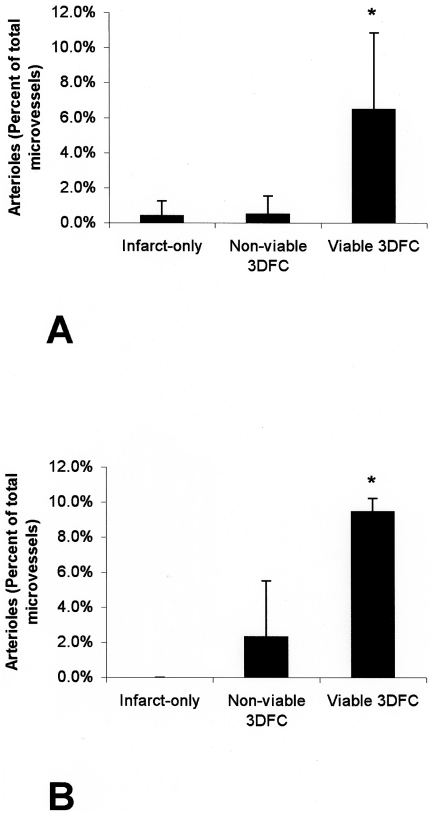

Figure 4. Arterioles as percent of total microvessels at 14 (A) and 30 (B) days. *$P \leq 0.05$.

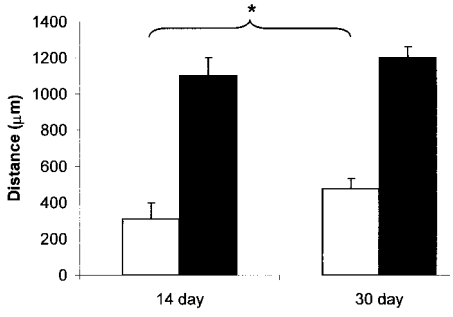

Figure 5. Depth of angiogenic effect of viable 3DFC at 14 and 30 days. Solid bars, ventricle wall thickness; open bars, depth of angiogenic effect. *$P \leq 0.05$.

growth factors, and extracellular matrix proteins including, but not limited to, VEGF, platelet-derived growth factor A chain, hepatocyte growth factor, keratinocyte growth factor, interleukin 6, interleukin 8, transforming growth factor-β_1, collagen protein,[18] and angiopoietin-1.[18,27]

In contrast, a number of investigators have focused on the therapeutic use of individual growth factors, such as either VEGF or bFGF, to stimulate the revascularization of ischemic cardiac tissues.[7,6] These growth factors have been targeted for preclinical and clinical studies because of their well-described angiogenic potential. Further research has shown that vessel development after VEGF treatment alone supports a leaky, immature, and hemorrhagic capillary vasculature.[30] In separate experiments from the same study, the coexpression of angiopoietin-1 and VEGF stimulated the formation of a leakage-resistant vasculature, with an additive effect on angiogenesis, and led to the development of a more mature microvasculature that was characterized by the presence of larger-diameter vessels, capillaries, and postcapillary venules.[30] Collectively, these angiogenic factor studies indicate that a single protein may not be ideal for the stimulation of an appropriate microvasculature. Therefore, the potential exists that multiple angiogenic factors produced by viable 3DFC (eg, VEGF and angiopoietin-1) may collectively contribute to the formation of a mature new vascular bed that serves the physiological needs of ischemic cardiac tissues.

These present studies demonstrate a potential clinical use for viable 3DFC as a cardiac implant to stimulate an angiogenic response and revascularize infarcted cardiac tissues. Because complete revascularization cannot be achieved in up to 37% of patients undergoing CABG,[31] viable 3DFC may serve as a possible adjunct to CABG or PTCA in clinical cases in which underperfused myocardial areas are not amenable to grafting or endovascular therapy because of diffuse disease or small vessel size.

References

1. Schwartz RS, Holmes DR Jr, Topol EJ. The restenosis paradigm revisited: an alternative proposal for cellular mechanisms. *J Am Coll Cardiol*. 1992;20:1284–1293.
2. Hlatky MA. Analysis of costs associated with CABG and PTCA. *Ann Thorac Surg*. 1996;61:S30–S32.
3. Canver CC. Conduit options in coronary artery bypass surgery. *Chest*. 1995;108:1150–1155.
4. Chu VF, Giaid A, Kuang JQ, et al. Thoracic Surgery Directors Association Award. Angiogenesis in transmyocardial revascularization: comparison of laser versus mechanical punctures. *Ann Thorac Surg*. 1999; 68:301–307.
5. Lutter G, Yoshitake M, Takahashi N, et al. Transmyocardial laser-revascularization: experimental studies on prolonged acute regional ischemia. *Eur J Cardiothorac Surg*. 1998;13:694–701.
6. Laham RJ, Sellke FW, Edelman ER, et al. Local perivascular delivery of basic fibroblast growth factor in patients undergoing coronary bypass surgery: results of a phase I randomized, double-blind, placebo-controlled trial. *Circulation*. 1999;100:1865–1871.
7. Symes JF, Losordo DW, Vale PR, et al. Gene therapy with vascular endothelial growth factor for inoperable coronary artery disease. *Ann Thorac Surg*. 1999;68:830–836.
8. Rajanayagam MA, Shou M, Thirumurti V, et al. Intracoronary basic fibroblast growth factor enhances myocardial collateral perfusion in dogs. *J Am Coll Cardiol*. 2000;35:519–526.
9. Horvath KA, Chiu E, Maun DC, et al. Up-regulation of vascular endothelial growth factor mRNA and angiogenesis after transmyocardial laser revascularization. *Ann Thorac Surg*. 1999;68:825–829.
10. Terp K, Koudahl V, Veien M, et al. Functional remodelling and left ventricular dysfunction after repeated ischaemic episodes: a chronic experimental porcine model. *Scand Cardiovasc J*. 1999;33:265–273.
11. Atkins BZ, Hueman MT, Meuchel JM, et al. Myogenic cell transplantation improves in vivo regional performance in infarcted rabbit myocardium. *J Heart Lung Transplant*. 1999;18:1173–1180.
12. Schwarz ER, Speakman MT, Patterson M, et al. Evaluation of the effects of intramyocardial injection of DNA expressing vascular endothelial growth factor (VEGF) in a myocardial infarction model in the rat: angiogenesis and angioma formation. *J Am Coll Cardiol*. 2000;35:1323–1330.
13. Sakai T, Li RK, Weisel RD, et al. Autologous heart cell transplantation improves cardiac function after myocardial injury. *Ann Thorac Surg*. 1999;68:2074–2080.
14. Kumashiro H, Kusachi S, Moritani H, et al. Establishment of a long-surviving murine model of myocardial infarction: qualitative and quantitative conventional microscopic findings during pathological evolution. *Basic Res Cardiol*. 1999;94:78–84.
15. Unger EF. Experimental evaluation of coronary collateral development. *Cardiovasc Res*. 2001;49:497–506.
16. Operschall C, Falivene L, Clozel JP, et al. A new model of chronic cardiac ischemia in rabbits. *J Appl Physiol*. 2000;88:1438–1445.
17. Naughton G, Mansbridge J, Gentzkow G. A metabolically active human dermal replacement for the treatment of diabetic foot ulcers. *Artif Organs*. 1997;21:1203–1210.
18. Mansbridge J, Liu K, Pinney E, et al. Growth factors secreted by fibroblasts: role in healing diabetic foot ulcers. *Diabetes Obes Metab*. 1999; 1:265–279.
19. Kumashiro H, Kusachi S, Moritani H, et al. Establishment of a long-surviving murine model of myocardial infarction: qualitative and quantitative conventional microscopic findings during pathological evolution. *Basic Res Cardiol*. 1999;94:78–84.
20. Weidner N, Semple JP, Welch WR, et al. Tumor angiogenesis and metastasis: correlation in invasive breast carcinoma. *N Engl J Med*. 1991;324:1–8.
21. Rendell MS, Finnegan MF, Pisarri T, et al. A comparison of the cutaneous microvascular properties of the spontaneously hypertensive rat and the Wister-Kyoto rat. *Comp Biochem Physiol*. 1999;122:399–406.
22. Clark RAF. Overview and general considerations of wound repair. In: Clark RAF, Henson PM, eds. The Molecular and Cellular Biology of Wound Repair. New York, NY: Plenum Press; 1996:3–33.
23. Sunderkotter C, Steinbrink K, Goebeler M, et al. Macrophages and angiogenesis. *J Leukoc Biol*. 1994;55:410–422.
24. Sunderkotter C, Goebeler M, Schulze-Osthoff K, et al. Macrophage-derived angiogenesis factors. *Pharmacol Ther*. 1991;51:195–216.
25. Schaper W. Angiogenesis in the adult heart. *Basic Res Cardiol*. 1991; 2(suppl 86):51–56.
26. Beck CS, Tichy VL. The production of a collateral circulation to the heart. *Am Heart J*. 1935;10:849–873.
27. Pinney E, Liu K, Sheeman B, et al. Human three-dimensional fibroblast cultures express angiogenic activity. *J Cell Physiol*. 2000;183:74–82.
28. Jiang WG, Harding KG. Enhancement of wound tissue expansion and angiogenesis by matrix-embedded fibroblast (Dermagraft): a role of hepatocyte growth factor/scatter factor. *Int J Mol Med*. 1998;2:203–210.
29. Naughton G, Mansbridge J, Gentzkow G. A metabolically active human dermal replacement for the treatment of diabetic foot ulcers. *Artif Organs*. 1997;21:1203–1210.
30. Thurston G, Suri C, Smith K, et al. Leakage-resistant blood vessels in mice transgenically overexpressing angiopoietin-1. *Science*. 1999;286: 2511–2514.
31. Levin DC, Beckmann CF, Sos TA, et al. Incomplete myocardial reperfusion despite a patent coronary bypass: a generally unrecognized shortcoming of the surgical approach to coronary artery disease. *Radiology*. 1982;142:317–321.